

## Synthesis of Silver Nanoparticles by *Bacillus stearothermophilus* Using Gamma Radiation and Their Antimicrobial Activity

<sup>1</sup>A.I. El-Batal, <sup>2</sup>M.A. Amin, <sup>3</sup>Mona M.K. Shehata and <sup>1</sup>Merehan M.A. Hallol

<sup>1</sup>Drug Radiation Research Department, Biotechnology Division, National Center for Radiation Research and Technology (NCRRT), Atomic Energy Authority, Cairo, Egypt

<sup>2</sup>Microbiology and Immunology Department, Faculty of Pharmacy, Cairo University

<sup>3</sup>Drug Microbiology Laboratory, Drug Radiation Research Department, National Center for Radiation Research and Technology (NCRRT), Atomic Energy Authority, Cairo, Egypt

**Abstract:** *Bacillus stearothermophilus* culture supernatant was used for preparation of silver nanoparticles (AgNPs) by reduction of silver ions via nitrate reductase enzyme which was optimized using Response Surface Methodology (RSM). The optimized conditions for nitrate reductase activity were as follows; medium containing; (%) glucose: 0.1, peptone: 1, yeast extract: 0.4, KNO<sub>3</sub>: 0.4 also, pH: 7.5, temp: 25°C and incubation period 3 days with maximum nitrate reductase activity of (731.24 U/ml). AgNPs were characterized by UV-Vis spectroscopy, Transmission Electron Microscopy (TEM), Dynamic Light Scattering (DLS) and Fourier Transform Infrared Spectroscopy (FT-IR). Effect of gamma radiation on bacterial free filtrate before and after mixing with Ag<sup>+</sup> in aqueous solutions was investigated. Increasing of gamma radiation doses from 0.25 up to 3 kGy enhanced the formation of AgNPs. The antimicrobial activity of AgNPs was investigated against some pathogenic multidrug-resistant strains of yeast, Gram-negative and Gram-positive bacteria using the Kirby-Bauer method. AgNPs effectively inhibited microbial growth in the order of *Candida* spp>Gram-positive bacteria>Gram-negative bacteria. Minimum inhibitory concentrations (MICs) and minimum lethal concentrations (MLCs) of AgNPs were determined for selected strains by a broth dilution method. The results showed that the lowest MIC and MLC of AgNPs was 100 and 200ppm for *Candida parapsilosis*, respectively. This *in vitro* study demonstrated the effectiveness of the synthesized AgNPs as a new tool in combating against infectious diseases.

**Key words:** Silver nanoparticles % Nitrate reductase % Response surface methodology % Gamma-irradiation % Antimicrobial activity % Multidrug –resistant strains

### INTRODUCTION

Synthesis of nanoparticles as an emerging highlight of the intersection of nanotechnology and biotechnology has received increasing attention due to a growing need to develop environmentally-benign technologies in material synthesis. The metallic nanoparticles are the most promising as they show good antibacterial properties due to their large surface area to volume ratio, which is coming up as the current interest in the researchers due to the growing microbial resistance against metal ions, antibiotics and the development of resistant strains [1].

Silver has long been known to exhibit a strong toxicity to a wide range of 116 microorganisms [2] for these reasons silver-based compounds have been used extensively in many bactericidal applications [3, 4]. Several salts of silver and their derivatives are commercially employed as antimicrobial agents. The bactericidal effect of silver ions on microorganisms is very well known; however, the bactericidal mechanism is only partially understood. It has been proposed that ionic silver strongly interacts with thiol groups of vital enzymes and inactivates them [3]. Experimental evidence suggests that DNA loses its replication ability once the bacteria have been treated with

silver ions. Other studies have shown evidence of structural changes in the cell membrane as well as the formation of small electron-dense granules formed by silver and sulfur [5]. Metal particles in the nanometer size range exhibit physical properties that are different from both the ion and the bulk material. This makes them exhibit remarkable properties such as increased catalytic activity due to morphologies with highly active facets [5]. Microorganisms, such as bacteria and fungi, now play an important role in the remediation of toxic metals through the reduction of the metal ions [6]. Response Surface Methodology (RSM) is a collection of statistical and mathematical techniques useful for developing, improving and optimizing processes [7, 8]. RSM is a well-known method applied in the optimization of medium constituents and other critical variables responsible for the production of biomolecules [9, 10]. In addition to analyzing the effects of the independent variables, this experimental methodology generates a mathematical model that accurately describes the overall process. It has been successfully applied to optimize the conditions in food, chemical and biological processes [7, 11]. The conventional practice of single factor optimization by maintaining other factors at an unspecified constant level does not depict the combined effect of all the factors involved. The one factor at a time method requires a large number of experiments to determine optimum levels, which is tedious and time consuming [9, 12]. Optimizing all the effecting parameters can eliminate these limitations of a single factor optimization process collectively by statistical experimental design using RSM. Gamma-irradiation synthesis of metallic nanoparticles has been also employed as one of the most promising methods to produce AgNPs due to some important advantages [13-16]. As compared to conventional chemical/photochemical techniques, the radiochemical process can be performed to reduce Ag<sup>+</sup> ions at the ambient temperature without using excessive reducing agents or producing unwanted by-products of the reductant. Moreover, reducing agent can be uniformly distributed in the solution and AgNPs are produced in highly pure and stable form [17]. The development of new resistant strains of bacteria to current antibiotics has become a serious problem in public health; therefore, there is a strong incentive to develop new bactericides [18, 19].

The aim of this study was to use the culture cell free supernatant of the non-pathogenic *Bacillus stearothermophilus* for the synthesis of AgNPs from the standpoint of ease of mass production and safety in

handling the organism. The current work involved the optimization of medium components for nitrate reductase production by *B. stearothermophilus* to enhance the synthesis of AgNPs. Also, the antimicrobial activity of the AgNPs synthesized against selected strains of pathogenic multidrug-resistant bacteria and yeast causing life-threatening infections was evaluated. The antimicrobial activity was assessed by measuring the diameter of inhibition zones tested with the Kirby-Bauer diffusion method, by determining the minimum inhibitory concentration (MIC) using the standard dilution macromethod and by determining the minimum lethal concentration (MLC).

## MATERIALS AND METHODS

**Chemicals:** All the media, chemicals, reagents and silver nitrate used in the following experiments were of analytical grade and used without further purification.

**Organism and Culture Maintenance:** The culture of *Bacillus stearothermophilus* was obtained from the Drug Radiation Research Department at National Center for Radiation Research and Technology (NCRRT), Atomic Energy Authority, Cairo, Egypt. The culture was maintained at 4°C in nutrient agar plates. The culture was maintained by continuous sub-culturing every 2 weeks.

**Irradiation Source:** The process of irradiation was carried out at NCRRT. Irradiations were performed within a gamma-irradiation system using Co-60 source (Gamma cell 4000-A-India), at a dose rate of 3.31 kGy/hr at the time of the experiments.

**Estimation of Nitrate Reductase Activity:** *Bacillus stearothermophilus* was grown in 50 ml medium containing; (%) glucose:0.1, yeast extract:0.4, peptone:1 and KNO<sub>3</sub>:0.4, in 250 ml Erlenmeyer flasks at 25°C with shaking (200 rpm) for 24 hrs using (LAB-Line® Orbit Environ) shaker. Cell free supernatant was prepared by separation of bacteria which were collected by centrifugation using (Hettich Universal 16R cooling centrifuge) at 6,000 rpm for 10 minutes at 6°C. In our study, the seven factors for optimization fermentation processes: glucose, peptone, yeast extract, KNO<sub>3</sub>, pH, temperature and incubation period were optimized using RSM to improve microbial production of nitrate reductase enzyme. Nitrate reductase activity was estimated by modified procedure based on the method of Vaidyanathan *et al.* [20]. The cell free supernatant obtained was used as

the crude enzyme. The protocol uses 25 mM potassium phosphate buffer with 30mM potassium nitrate and 0.05 mM ethylenediaminetetraacetic acid at pH 7.3 as the enzyme substrate. 100  $\mu$ l of enzyme was allowed to react with 1.8 ml of substrate solution and the reaction was supported by 100  $\mu$ l of 2.5 mM  $\beta$ -nicotinamide adenine dinucleotide reduced form solution ( $\beta$ -NADH). The reaction mixture was incubated at 30°C for 5min. Then the reaction was terminated immediately by adding and swirling 1ml of 58mM sulphanilamide solution in 3M HCl. Then 1ml of 0.77mM N-(1-naphthyl) ethylenediamine dihydrochloride solution (NED) was added and mixed by swirling. The color formation was noticed after 5 min of incubation of the mixture. The absorbency was recorded at 540 nm. Units are defined as micromoles of nitrite produced per min [20].

#### **Synthesis and Characterization of Silver Nanoparticles:**

Synthesis of AgNPs was carried out according to the method described by Kalishwaralal *et al.* [6] and Vaidyanathan *et al.* [20] with slight modification. In Erlenmeyer flasks, cell supernatant of optimum medium (100 ml) mixed with 1mM silver nitrate ( $\text{AgNO}_3$ ) and incubated for 10 hr. The absorption spectrum of the sample was recorded on JASCO V-560 UV-visible spectrophotometer operating at a resolution of 1 nm. In typical experiment, cell supernatant was exposed to gamma irradiation before and after mixing with  $\text{AgNO}_3$  solution at doses 0.25, 0.50, 0.75, 1.00, 1.25, 1.50, 1.75, 2.00 and 3.00 kGy at room temperature. After irradiation the produced AgNPs were characterized by the UV-vis spectroscopy, Dynamic Light Scattering (DLS), Transmission Electron Microscopy (TEM) and the Fourier Transform Infrared (FT-IR) spectroscopy.

**UV/vis Spectral Analysis:** UV/vis spectra of AgNPs were recorded as a function of wavelength using JASCO V-560. UV/vis spectrophotometer from 200-900 nm operated at a resolution of 1 nm.

**Dynamic Light Scattering (DLS):** Average particle size and size distribution were determined by PSS-NICOMP 380-ZLS particle sizing system St. Barbara, California, USA.

**Fourier Transform Infra-Red Spectroscopy (FT-IR):** FT-IR measurements were carried out in order to obtain information about chemical groups present around AgNPs for their stabilization and understand the transformation of functional groups due to reduction

process. The measurements were carried out using JASCO FT/IR-3600 infra-red spectrometer by employing KBr pellet technique.

**Transmission Electron Microscopy (TEM):** The size and morphology of the synthesized nanoparticles were recorded by using TEM model JEOL electron microscope JEM-100 CX. TEM studies were prepared by drop coating silver nanoparticles onto carbon-coated TEM grids. The film on the TEM grids were allowed to dry, the extra solution was removed using a blotting paper.

**Atomic Absorption Spectrophotometry:** Silver nanoparticles concentration assessment using UNICAM939 Atomic Absorption Spectrophotometry, England, equipped with deuterium background correction. All solutions were prepared with ultra pure water with a specific resistance 18  $\Omega$ /cm.

#### **Optimization of Medium Components for Nitrate**

**Reductase Production:** The influence of different factors on reductase productivity was evaluated using RSM with a total 97 runs. The independent variables include; glucose, peptone, yeast extract,  $\text{KNO}_3$ , pH, temperature and incubation period against the dependent variable nitrate reductase activity.

#### **Antimicrobial Study of the Synthesized Silver Nanoparticles**

**Determination of Zone of Inhibition (ZOI):** The AgNPs synthesized were tested for their antimicrobial activity by the agar well diffusion method [21] against different kinds of pathogenic multidrug resistant bacteria and yeast. The cultures of all strains used in this study were obtained from Drug Microbiology Laboratory, Drug Radiation Research Department, NCRRT, Cairo, Egypt. All the tested strains were isolated from clinical samples at the National Cancer Institute, Cairo, Egypt. The tested strains included; *Staphylococcus aureus* (MRSA), *Staphylococcus epidermidis*, *Staphylococcus warneri* and *Staphylococcus saprophyticus* as Gram+ve bacteria, *Acinetobacter baumannii/haemolyticus*, *Pseudomonas aeruginosa*, *Klebsiella pneumonia* and *Escherichia coli* as Gram-ve bacteria while, *Candida albicans*, *Candida parapsilosis*, *Candida tropicalis* and *Candida glabrata* were tested as yeast. Identification was carried out according to standard methods [22, 23] and then confirmed by using MicroScan WalkAway-96 SI System (Dade Behring, Germany) at the National Cancer Institute. Standardized suspension of each tested strain ( $10^8$  and  $10^6$

cfu/ml for bacteria and yeast, respectively) was swabbed uniformly onto sterile Muller-Hinton Agar (MHA) (Oxoid) plates using sterile cotton swabs. Wells of 10 mm diameter were bored into the agar medium using gel puncture. Using a micropipette, 100  $\mu$ l silver nanoparticles solution (200ppm) was added into each well. After incubation at 37°C for 24hrs, different levels of zone of inhibition were measured [24]. Tetracycline (antibacterial agent) and Amphotericin B (antifungal agent) served as positive controls for antimicrobial activity. The determinations were done in triplicate and the mean values  $\pm$  SD were presented.

**Determination of Minimum Inhibitory Concentration (MIC) and Minimum Lethal Concentration (MLC):** Five different strains; *Staphylococcus aureus* (MRSA) [coagulase positive staphylococci] and *Staphylococcus warneri* [coagulase negative staphylococci] as Gram+ve bacteria, *Acinetobacter baumannii/haemolyticus* and *Pseudomonas aeruginosa* as Gram-ve bacteria and *Candida parapsilosis* as a yeast were selected in this study. The MICs determinations were performed in Luria Bertani (LB) broth (BD BBL™) in duplicate using serial two-fold dilutions of AgNPs in concentrations ranging from 1600-0.049ppm, along with positive control tube (microorganism and nutrient) and negative control one (nutrient only) [25]. The MIC was determined after 24 h of incubation at 37°C with initial inoculums of 0.1 OD at 600 nm. The MIC is the lowest concentration of AgNPs that completely visually inhibits 99% growth of the tested microorganisms. The concentrations of AgNPs able to inhibit the visible growth of 50% and 90% of a population of microorganisms (MIC<sub>50</sub> and MIC<sub>90</sub>, respectively) were also determined. After MICs determinations of the AgNPs synthesized, aliquots of 50  $\mu$ l from all tubes in which no visible growth was observed were seeded in MHA plates not supplemented with AgNPs and were incubated for 24 h at 37°C. The MLC was defined as the lowest concentration of AgNPs with no growth on the MHA medium (i.e. kills 100% of the initial microbial population) [26]. The bacteriostatic and fungistatic effects of the AgNPs synthesized against the tested bacterial and yeast strains were represented by the MIC while, the bactericidal and fungicidal activities were represented by the MLC (MBC and MFC for bacteria and yeast strains, respectively). The antimicrobial study of the AgNPs synthesized including ZOI, MIC, MIC<sub>50</sub>, MIC<sub>90</sub> and MLC determinations was carried out for all the tested strains before and after their *in vitro* exposure to a dose level of 24.41 Gy gamma radiation. This was done to study the

antimicrobial activity of the AgNPs against microorganisms causing infections in radiotherapy treated cancer patients. 24.41Gy is a single dose biologically equivalent to the fractionated multiple therapeutic dose of 70 Gy/35 fractions given to cancer patients and was calculated by using the linear quadratic (LQ) formula [27]. The irradiation source used was <sup>137</sup>Cs Gamma cell 40, Atomic Energy of Canada Limited, Commercial Products located at the NCRRT, Atomic Energy Authority, Cairo, Egypt. The dose rate at the time of experiments was 0.774 rad /sec. All the antimicrobial studies were carried out at the Drug Microbiology Laboratory, NCRRT, Atomic Energy Authority, Cairo, Egypt.

**Statistical Analysis:** The results of optimization of medium components for nitrate reductase production were analyzed by using the software statistical version 6.0 (Statsoft inc.USA). The antimicrobial activity results were analyzed by using the statistical analysis system SAS (Version 9) by SAS Institute Inc. Cary, NC, USA.

## RESULTS AND DISCUSSION

**Synthesis of Silver Nanoparticles:** Aqueous Ag<sup>+</sup> ions were reduced to AgNPs when added to the cell free supernatant of *B. stearotheophilus* within 10 hr after incubation before optimization of media. During incubation, a color change was observed from whitish yellow to brown and the control showed no color change. The appearance of brown color in AgNO<sub>3</sub> treated flask is attributed to the Surface Plasmon Resonance (SPR) suggested the formation of AgNPs. A characteristic SPR band for AgNPs is obtained at 8 431 nm was done by spectrophotometric analysis indicating the presence of spherical or roughly spherical Ag nanoparticles (Fig. 1) [6]. The UV-Vis spectra absorbance as a function of time, at a concentration of 1 mM silver nitrate and 5 ml of cell free supernatant, indicated that the reaction was completed during the first 12 hours and further increase in time does not influence the formation of AgNPs as described in Fig. 2.

**Optimization of Medium Components for Nitrate Reductase Production:** In the present study, the highest value (731.24 U/ml) of nitrate reductase activity obtained was observed in the 60<sup>th</sup> run (Table 1) with the optimized conditions; (%) glucose: 0.1, peptone: 1, yeast extract: 0.4, KNO<sub>3</sub>: 0.4, initial medium pH: 7.5, incubation temperature: 25°C and incubation period 3 days. The optical density of synthesized silver nanoparticles showed no relation with

Table 1: The experimental conditions and the results of nitrate reductase activity (Combination of variables and Response in RSM design)

No. of run	Glucose g/l	Peptone g/l	Yeast extract g/l	Pot.nitrate g/l	pH	Temp °C	Incubation period day	Enzyme activity U/ml	OD at 8 430 nm of silver nanoparticles
1	1.5	15	3.5	3.5	7	30	2	295.6	1.5
2	2	20	3	3	6.5	25	1	566.21	2
3	2	10	3	4	7.5	35	1	176.6	1.9
4	1.5	15	3.5	3.5	7	30	2	295.6	1.5
5	1	10	4	4	6.5	25	1	126.35	1.9
6	1	20	3	4	7.5	35	1	172.3	1.4
7	2	20	4	3	7.5	25	1	493.42	1.9
8	1.5	15	3.5	3.5	7	30	2	295.6	1.8
9	1.5	15	3.5	3.5	8.41	30	2	601.6	1.4
10	1	10	4	3	7.5	25	1	435.77	1.9
11	2	10	4	4	6.5	35	1	316.77	1.3
12	1.5	15	3.5	3.5	7	30	2	295.6	1.8
13	2	10	3	3	7.5	35	3	102.16	1.8
14	2	10	3	3	7.5	25	1	52.67	1.4
15	2	10	4	3	7.5	35	1	399.5	2
16	2.91	15	3.5	3.5	7	30	2	533.3	1.9
17	1	20	4	4	6.5	35	1	523.73	1.2
18	1.5	15	3.5	3.5	7	30	2	295.6	1.6
19	1.5	15	3.5	3.5	7	30	4.83	281.1	1.4
20	1.5	15	3.5	3.5	7	30	2	295.6	1.9
21	1.5	15	3.5	3.5	7	30	2	295.6	1.7
22	2	20	3	3	6.5	35	3	227.7	2
23	1.5	15	3.5	4.91	7	30	2	435.8	1.1
24	1	10	4	3	6.5	25	3	571.677	1.4
25	2	10	3	4	6.5	35	3	259.2	2
26	1.5	15	3.5	3.5	7	30	2	295.6	1.8
27	1	20	4	3	6.5	35	3	360.6	1.6
28	2	10	3	3	6.5	35	1	420.33	1.7
29	1	20	4	3	6.5	25	1	273.3	1
30	1	20	3	4	6.5	25	1	142.06	1.1
31	1.5	15	3.5	3.5	7	30	2	295.6	1.2
32	2	20	4	4	7.5	35	1	244.7	1.3
33	1	20	4	4	7.5	35	3	370.012	1.9
34	2	20	3	4	7.5	35	3	271.66	1.7
35	2	20	4	4	6.5	35	3	167.98	1.5
36	2	10	4	3	7.5	25	3	542.86	2
37	1	10	4	3	6.5	35	1	215.8	1.5
38	1.5	15	3.5	3.5	7	30	2	295.6	1.9
39	2	20	4	3	6.5	35	1	186.5	1.7
40	1	10	3	4	7.5	25	1	169.63	1.5
41	2	20	4	4	7.5	25	3	525.22	1.4
42	2	20	3	3	7.5	25	3	555.28	1.2
43	1	20	3	3	6.5	25	3	427.33	1.6
44	1.5	15	3.5	3.5	7	30	2	295.6	1.3
45	2	20	4	4	6.5	25	1	524.22	1.7
46	1.5	15	3.5	3.5	7	30	2	295.6	1.5
47	1	10	4	4	6.5	35	3	325.79	2
48	1	10	3	4	6.5	25	3	529.69	1.1
49	1	20	3	4	6.5	35	3	165.4	1.6
50	1	10	4	3	7.5	35	3	219.8	1.9
51	2	20	3	4	6.5	35	1	263.5	1.3
52	1	20	3	3	6.5	35	1	426.9	1.8
53	2	10	3	3	6.5	25	3	441.5	1.4
54	1.5	15	3.5	3.5	7	30	2	295.6	1.7
55	1	10	3	3	7.5	35	1	340.8	1.4

Table 1: Continued

56	2	20	3	4	7.5	25	1	102.36	1.2
57	1	10	3	3	7.5	25	3	307.16	2
58	2	10	3	4	6.5	25	1	56.65	1.1
59	1	20	4	4	7.5	25	1	231.76	1.9
60	1	10	4	4	7.5	25	3	731.24	2.2
61	2	10	4	4	7.5	35	3	120.46	1.8
62	1.5	15	3.5	3.5	7	30	2	295.6	1.3
63	2	10	4	4	7.5	25	1	718.67	1.7
64	1.5	15	3.5	3.5	7	30	2	295.6	1.4
65	1	20	3	4	7.5	25	3	212.22	1.6
66	1	20	3	3	7.5	25	1	290.4	1.5
67	1	10	3	3	6.5	35	3	205.6	1.5
68	2	20	4	3	6.5	25	3	700.87	2
69	1.5	15	3.5	3.5	7	30	2	295.6	1
70	2	20	3	3	7.5	35	1	219.6	1.1
71	2	20	3	4	6.5	25	3	368.24	1.3
72	1	20	4	3	7.5	25	3	695.287	1.2
73	2	10	4	4	6.5	25	3	693.54	1.4
74	1.5	15	3.5	3.5	7	30	2	295.6	1.6
75	1.5	15	3.5	3.5	7	30	2	295.6	1.5
76	1	10	3	3	6.5	25	1	64.35	1.7
77	1	10	4	4	7.5	35	1	326.3	1.9
78	1.5	15	3.5	3.5	7	30	2	295.6	1.8
79	1.5	15	4.91	3.5	7	30	2	370.4	2
80	0.086	15	3.5	3.5	7	30	2	391.19	1.8
81	1.5	0.858	3.5	3.5	7	30	2	346.86	1.9
82	1.5	15	3.5	3.5	5.58	30	2	380.8	1.7
83	2	10	4	3	6.5	25	1	488.3	1.5
84	1	20	3	3	7.5	35	3	180.18	1.6
85	1.5	15	3.5	3.5	7	30	2	295.6	1.4
86	1	20	4	4	6.5	25	3	644.33	1.2
87	1.5	15	2.08	3.5	7	30	2	491.5	1.2
88	1.5	29.14	3.5	3.5	7	30	2	530.5	1.1
89	1	10	3	4	6.5	35	1	506.48	1
90	1.5	15	3.5	3.5	7	30	2	295.6	1.2
91	1.5	15	3.5	3.5	7	30	2	295.6	1.6
92	2	10	3	4	7.5	25	3	215	1.4
93	1	20	4	3	7.5	35	1	235.3	1.8
94	1	10	3	4	7.5	35	3	473.7	2
95	2	20	4	3	7.5	35	3	185.26	1.9
96	2	10	4	3	6.5	35	3	119.69	1.7
97	1.5	15	3.5	2.08	7	30	2	172.01	1.5

Table 2: Regression analysis of the RSM design

Source	df	Sum of Squares	Mean Square	F Ratio
Model	35	1632348.1	46638.5	3.6707
Error	61	775040.2	12705.6	Prob > F
C. Total	96	2407388.3	--	<0.0001*

df : degree of freedom , \* :Significant

the activity of nitrate reductase enzyme which may indicate presence of other reductases which may affect the synthesis. To construct a first order model that can predict the nitrate reductase activity (dependent variable) as a function of physical parameters (independent variables) as shown in Table 2. ANOVA consists of classifying and cross classifying statistical results and

testing whether the means of a specified classification differ significantly. This was carried by Fisher's statistical test for the analysis of variance. The Fischer's F-test showed a value of 3.6707 which is much greater than that of the F tabulated 0.0001 and that demonstrates that the model terms are significant [20]. The model equation fitted by regression analysis is given by:

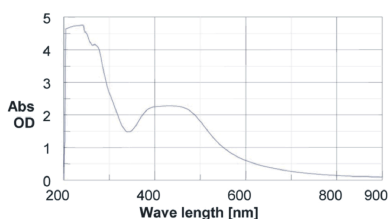


Fig. 1: UV VIS-Spectrum of Silver nanoparticles

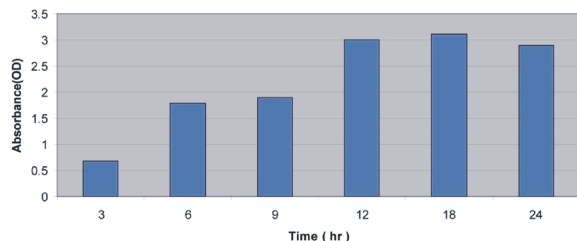


Fig. 2: Effect of time on formation of AgNPs

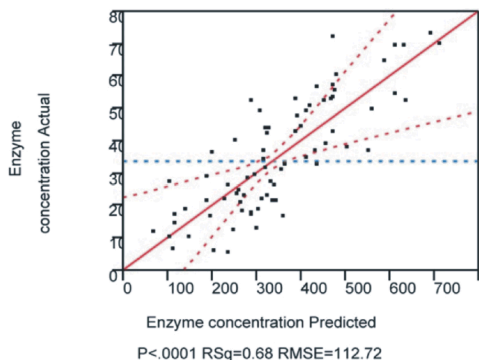


Fig. 3: Response enzyme concentration (U/ml) actual by predicted plot

Actual = 295.6 + 2.84 Glucose + 9.99 Peptone + 43.25 Yeast extract + 5.87 Potassium nitrate - 4.61 pH - 65.11 Temp + 34.46 incubation period + 10.59 Glucose \* Peptone + 7.13 Glucose \* Yeast extract - 4.06 Peptone \* Yeast extract - 16.84 Glucose \* Potassium nitrate - 29.88 Peptone \* Potassium nitrate + 18.92 Yeast extract \* Potassium nitrate - 11.85 Glucose \* pH - 15.23 Peptone \* pH + 22.90 Yeast extract \* pH - 1.73 Potassium nitrate \* pH - 39.99 Glucose \* Temp - 14.61 Peptone \* Temp - 62.34 Yeast extract \* Temp + 24.28 Potassium nitrate \* Temp - 4.91 pH \* Temp - 26.13 Glucose \* incubation period + 1.83 Peptone \* incubation period + 4.11 Yeast extract \* incubation period + 11.53 Potassium nitrate \* incubation period - 0.16 pH \* incubation period - 72.58 Temp \* incubation period + 20.83 Glucose \* Glucose + 17.89 Peptone \* Peptone + 16.92 Yeast extract \* Yeast extract + 1.04 Potassium nitrate \* Potassium nitrate + 24.45 pH \* pH - 24.79 Temp \* Temp - 14.00 incubation period \* incubation period.

The model determination coefficient  $R^2$  (0.678058) suggested that the fitted model could explain 67.8% of the total variation. This implies a satisfactory representation of the process by the model (Fig. 3). Both the  $t$ -value and  $p$ -value statistical parameters were used to confirm the significance of factors studied. The  $t$ -value that measured how large the coefficient is in relationship to its standard error was obtained by dividing each coefficient by its standard error. The  $p$ -value is the chance of getting a larger  $t$ -value (in absolute value) by chance alone. The larger the magnitude of the  $t$ -value and smaller the  $p$ -value, more significant is the corresponding coefficient [28]. The results presented in Table 3 demonstrate that the nitrate reductase activity was significantly affected by yeast extract, temp and incubation period. Yeast extract at high level 0.4 showed higher nitrate reductase activity. Temperature at low level 25°C showed higher nitrate reductase activity. Nitrate reductase activity was higher at the high level of incubation period (3 days). Also, significant interaction of incubation period and temperature, peptone and potassium nitrate, glucose and temp, yeast extract and temp was noted (Fig. 4). The biggest advantage of this study based on enzyme is the development of a new approach for the synthesis of nanomaterials.

**Characterization of Silver Nanoparticles:** The dispersions of silver nanoparticles display intense colors due to the Plasmon resonance absorption. The surface of a metal is like plasma, having free electrons in the conduction band and positively charged nuclei. Surface Plasmon Resonance (SPR) is a collective excitation of the electrons in the conduction band; near the surface of the nanoparticles. Electrons are limited to specific vibrations modes by the particle's size and shape. Therefore, metallic nanoparticles have characteristic optical absorption spectrum in the UV-visible region. As shown in Fig. 1, UV-visible spectrum of AgNPs was strong, broad peak and located between 420 and 440nm. The broad peak at 8 431 nm is due to Surface Plasmons, which arise from the collective oscillations of valence electrons in the electromagnetic field of incident radiation and is the characteristic of Ag nanoparticles [29]. Treatment of bacterial cell free supernatant with different doses of gamma radiation before and after mixing with silver nitrate solution showed that the cell free supernatant irradiated after mixing with AgNO<sub>3</sub> solution was more effective than that of the cell supernatant irradiated before mixing with AgNO<sub>3</sub> solution in the formation of silver nanoparticles (Figs. 7 and 8). This can

Table 3: Regression coefficients for nitrate reductase activity under different physical conditions

Parameters	Coefficients	SE coefficients	t-value	p-value
Intercept	295.6	24.03177	12.30	<.0001*
Glucose(1,2)	2.8415222	12.60237	0.23	0.8224
Peptone(10,20)	9.9900545	12.60237	0.79	0.431
Yeast extract(3,4)	43.245293	12.60237	3.43	0.0011*
Potassium nitrate(3,4)	5.8721099	12.60237	0.47	0.6429
pH(6.5,7.5)	-4.609891	12.60237	-0.37	0.7158
Temp(25,35)	-65.11347	14.08988	-4.62	<.0001*
incubation period(1,3)	34.459469	14.08988	2.45	0.0174*
Glucose*Peptone	10.591375	14.08988	0.75	0.4551
Glucose*Yeast extract	7.1320937	14.08988	0.51	0.6146
Peptone*Yeast extract	-4.060125	14.08988	-0.29	0.7742
Glucose*Potassium nitrate	-16.84091	14.08988	-1.20	0.2366
Peptone*Potassium nitrate	-29.88356	14.08988	-2.12	0.0380*
Yeast extract*Potassium nitrate	18.915906	14.08988	1.34	0.1844
Glucose*pH	-11.84769	14.08988	-0.84	0.4037
Peptone*pH	-15.22678	14.08988	-1.08	0.2841
Yeast extract*pH	22.898938	14.08988	1.63	0.1093
Potassium nitrate*pH	-1.732625	14.08988	-0.12	0.9025
Glucose*Temp	-39.99278	14.08988	-2.84	0.0061*
Peptone*Temp	-14.61106	14.08988	-1.04	0.3038
Yeast extract*Temp	-62.34347	14.08988	-4.42	<.0001*
Potassium nitrate*Temp	24.282281	14.08988	1.72	0.0899
pH*Temp	-4.90575	14.08988	-0.35	0.7289
Glucose*incubation period	-26.12759	14.08988	-1.85	0.0685
Peptone*incubation period	1.8314375	14.08988	0.13	0.897
Yeast extract*incubation period	4.1100937	14.08988	0.29	0.7715
Potassium nitrate*incubation period	11.528094	14.08988	0.82	0.4164
pH*incubation period	-0.15575	14.08988	-0.01	0.9912
Temp*incubation period	-72.58191	14.08988	-5.15	<.0001*
Glucose*Glucose	20.830625	10.40606	2.00	0.0498*
Peptone*Peptone	17.885	10.40606	1.72	0.0907
Yeast extract*Yeast extract	16.91875	10.40606	1.63	0.1091
Potassium nitrate*Potassium nitrate	1.038125	10.40606	0.10	0.9209
pH*pH	24.45	10.40606	2.35	0.0220*
Temp*Temp	-24.79133	30.89129	-0.80	0.4254
incubation period*incubation period	-13.99576	15.24349	-0.92	0.3622

\*: Significant

be attributed to that, in case of samples irradiated before mixing the only one mechanism is due to reductase enzyme activity. In case of samples irradiated after mixing the nanoparticles synthesis is due to two mechanisms; the first is the reductase enzyme activity which was not nearly affected with irradiation at different doses (Fig. 5) and the second is radiolytic mechanism of gamma irradiation which increased the synthesis of silver nanoparticles (Fig. 6). The formation of AgNPs in case of radiation can be attributed to the radiolytic reduction which generally involves radiolysis of aqueous solutions that provides an efficient method to reduce metal ions. In the radiolytic method, when aqueous solutions are exposed to gamma rays, they create solvated electrons, which reduce the metal ions and the metal atoms eventually coalesce to form aggregates. The effect of

radiolytic reduction resulted in formation of AgNPs by radiolytic reactions and stabilization by prevention of aggregates formation by "capping". The peak shown in the Figs. 7 and 8 is relative to 0.75 kGy showed the maximum absorbance, after which the decrease in the SPR band intensity by increasing the irradiation dose more than 0.75 kGy may be attributed to the destructive effect of free radicals produced by gamma irradiation on the bioactive compounds (reductase enzyme) present in the extract [30].

The concentration of silver nitrate added strongly affects the reaction. As shown in Fig. 9, the absorbance intensity increases with increase in concentration (200, 300, 400, 800 and 1600 ppm ) in 5 ml of cell free supernatant, which indicates increased rate of reaction by increasing the concentration of silver nitrate used.



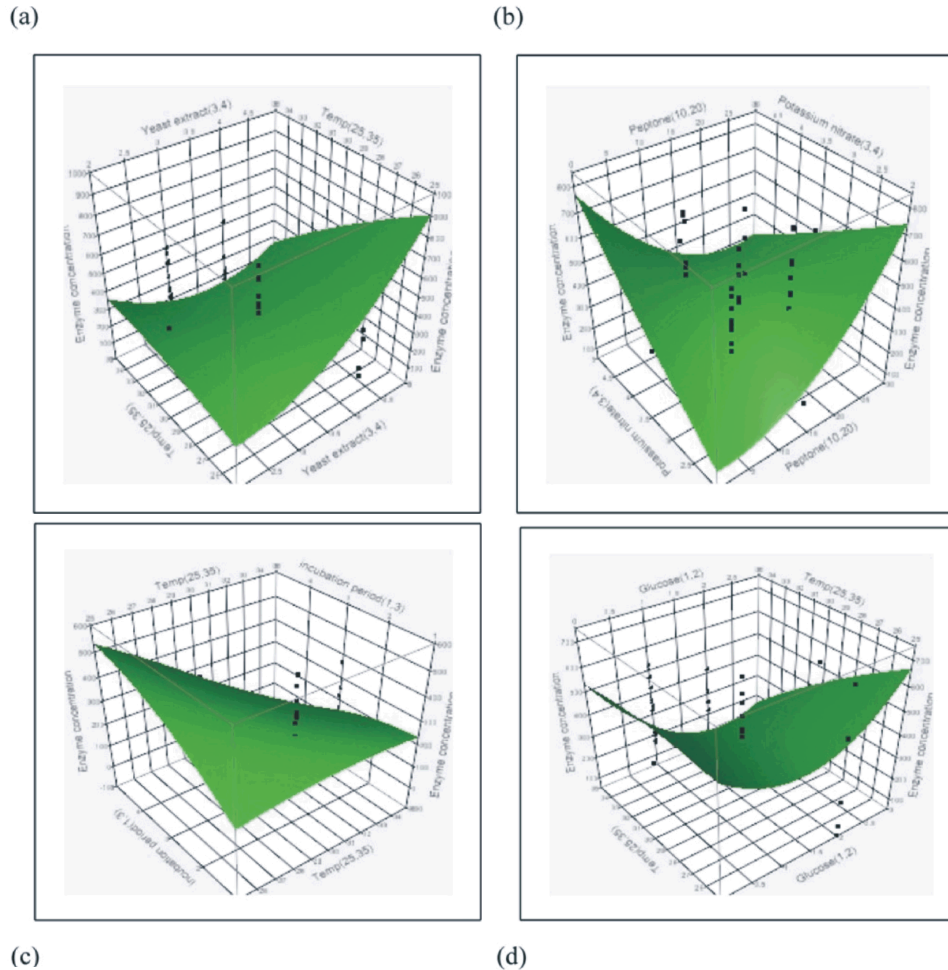


Fig. 4: Response surface graph illustrating the interaction between (a) Yeast extract and temp, (b) peptone and potassium nitrate, (c) incubation period and temp (d) glucose and temp relative to nitrate reductase activity by keeping the other components at this central level

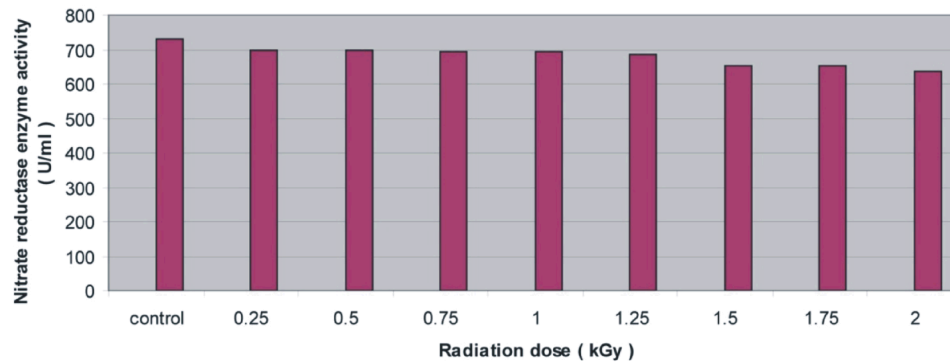


Fig. 5: Effect of different doses of gamma radiation (kGy) on nitrate reductase enzyme activity (U/ml)

TEM examination of the solution containing AgNPs demonstrated spherical particles within nano range ( $14 \pm 4$  nm) as shown in Fig. 10. The average particle size was determined by DLS method and was found to be 18.7 nm (Fig. 11). It was observed from the FT-IR spectrum

of AgNPs that the bands at  $1635.34/\text{cm}^{-1}$  (correspond to a primary amine NH band),  $1388.5/\text{cm}^{-1}$  and  $1118.51/\text{cm}^{-1}$  (correspond to a secondary amine NH band and primary amine CN stretch vibrations of the proteins, respectively) as shown in Fig. 12. The positions of these bands were

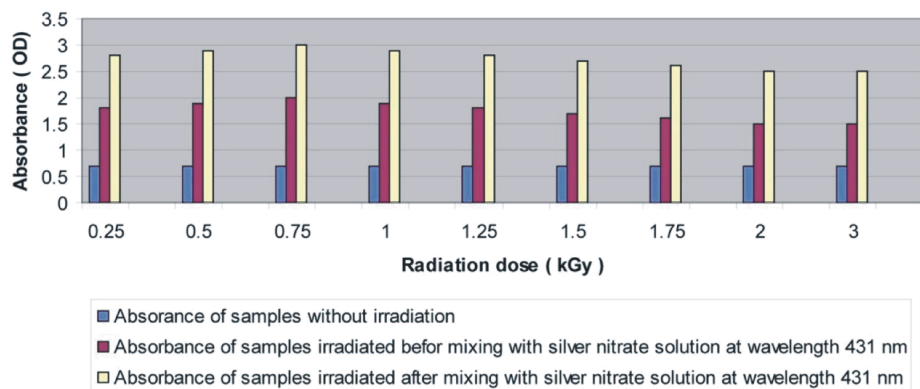


Fig. 6: Effect of different doses of gamma radiation (kGy) on formation of silver nanoparticles

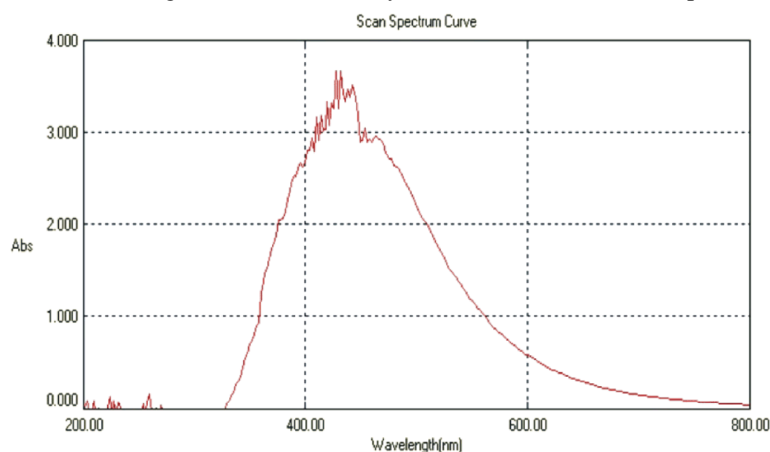


Fig. 7: UV-VIS Spectrum of cell free supernatant irradiated after mix with  $\text{AgNO}_3$  solution

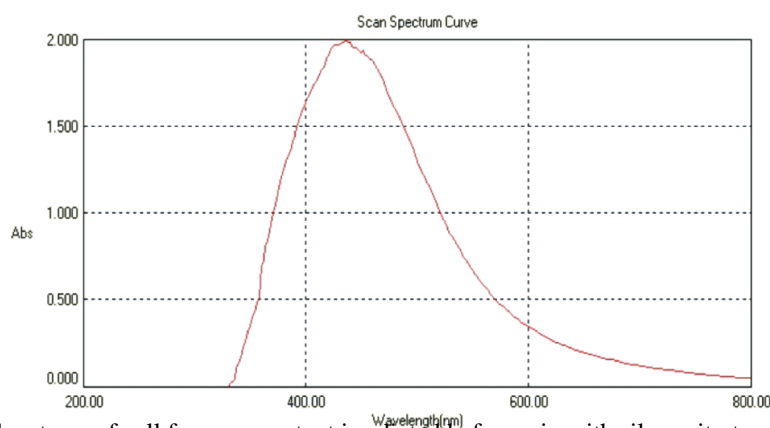


Fig. 8: UV-VIS Spectrum of cell free supernatant irradiated before mix with silver nitrate solution

close to that reported for native proteins. The FT-IR results indicated that the secondary structures of proteins were not affected as a consequence of reaction with  $\text{Ag}^+$  ions or binding with AgNPs. The band at  $1388.5/\text{cm}^{-1}$  is assigned to methylene scissoring vibration from the protein in the solution [31]. This evidence suggests that the release of extracellular protein molecules from

bacteria could possibly perform the function of the formation and stabilization of AgNPs in aqueous medium (Fig. 12).

**Antimicrobial Activity:** Synthesis of nanosized particles with antibacterial properties, which are called "nanoantibiotics", is of great interest in the development of new pharmaceutical products [1]. The use of AgNPs as

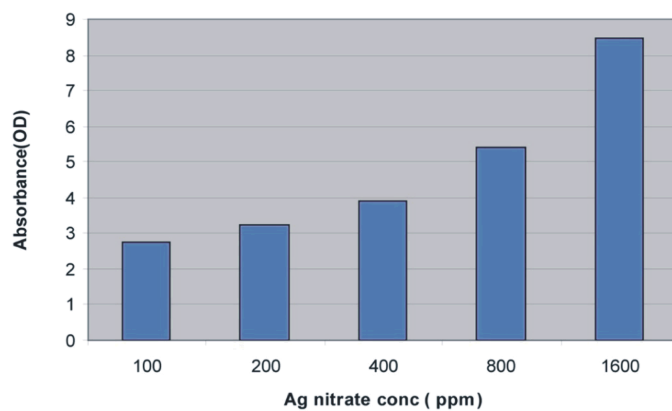


Fig. 9: Effect of  $\text{AgNO}_3$  concentration on formation of AgNPs

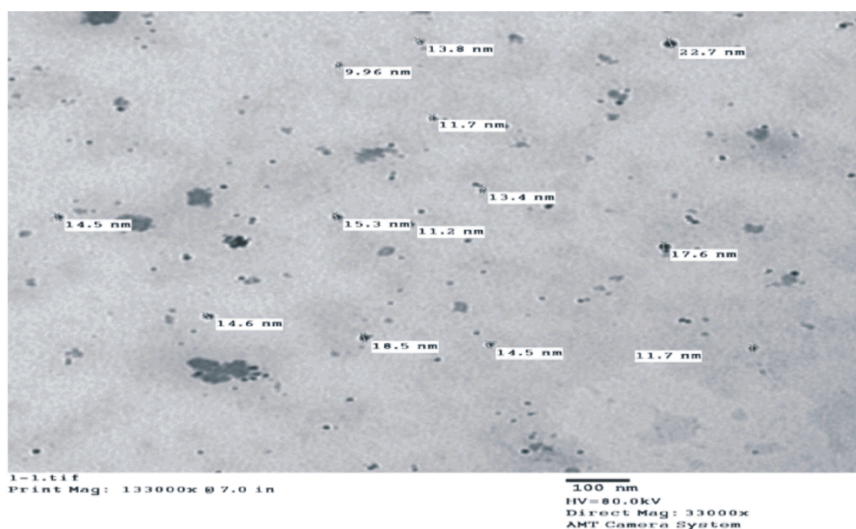


Fig. 10: TEM image for silver nanoparticles

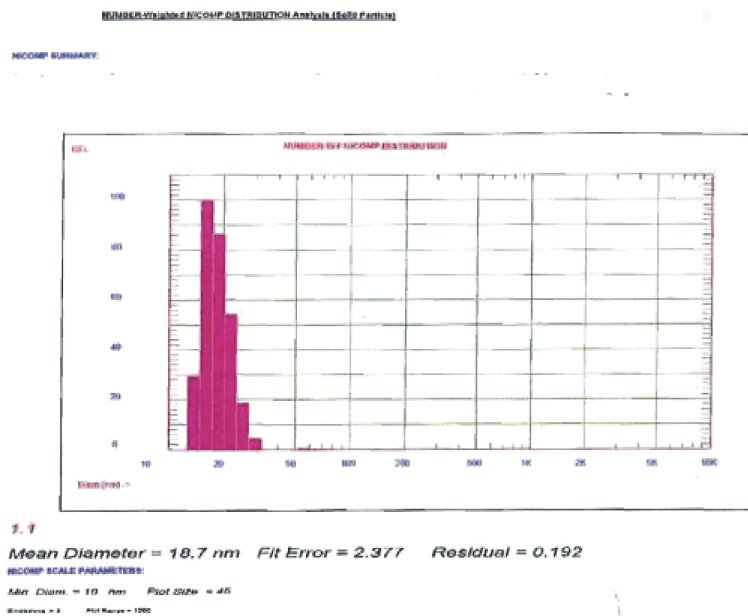


Fig. 11: Particle size distribution by DLS

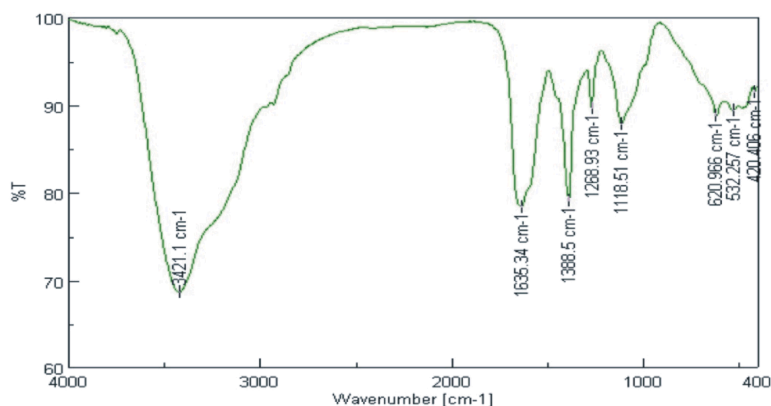


Fig. 12: FT-IR spectrum of fermented extract with silver nanoparticles

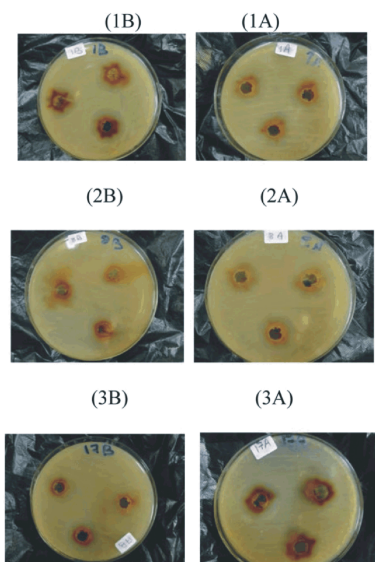


Fig. 13: Representative photographs showing antimicrobial activity of the synthesized silver nanoparticles against (1) *Candida albicans*, (2) *Staphylococcus epidermidis* and (3) *Staphylococcus warneri* before (B) and after (A) 24.41 Gy *in vitro* gamma irradiation respectively, according to the agar well diffusion method

an antibacterial agent is relatively new and has attracted significant attention in recent years [18, 32-34]. In this study, the antimicrobial activity of the AgNPs synthesized against different species of highly pathogenic multidrug resistant bacteria and yeast was investigated and AgNPs have been used as a comparable antimicrobial agent by antibacterial and antifungal drugs as Tetracycline and Amphotericin B, respectively. The average of particle size used in this study was  $14 \pm 4$  nm. The AgNPs synthesized were proved to have antimicrobial activity against all the tested

microorganisms (Table 4 and Fig. 13). The diameters of bacterial inhibition zones (mm) measured for MRSA, *Pseudomonas aeruginosa* and *E. coli* around  $27.67 \pm 0.577$ ,  $18.67 \pm 2.082$  and  $21.67 \pm 0.577$  before irradiation showed better antibacterial activity as compared to those reported by Guzman *et al.* [18] around  $11 \pm 1.0$ ,  $11 \pm 0.3$  and  $10 \pm 0.5$ , respectively with AgNPs mean diameter of  $14 \pm 5$ . Using the standard dilution macromethod, the MIC, MIC<sub>50</sub>, MIC<sub>90</sub> and MLC values of the AgNPs for the selected strains are summarized in Table 5. The values of MIC of the AgNPs synthesized against the tested clinical isolates showed a considerable antimicrobial activity; (200 ppm) for MRSA and *Staphylococcus warneri* and (100 ppm) for *Candida parapsilosis*. The lowest antimicrobial effect (400 ppm) was observed for *Acinetobacter baumannii/haemolyticus* & *Pseudomonas aeruginosa*. The results of antibacterial activity against MRSA before and after *in vitro* gamma irradiation were better as compared to study done earlier by Ayala-Nunez *et al.* [35] who reported MIC and MBC values of AgNPs around 1800 ppm and 2700 ppm, respectively.

The inhibitory impact of the AgNPs on each microorganism is specific and differs from one to another before and after *in vitro* gamma irradiation. The mechanism of inhibitory action of AgNPs on microorganisms suggests that upon treatment, DNA loses its replication ability and expression of ribosomal subunit protein, as well as other cellular proteins and enzymes essential to ATP production becomes inactivated [36]. Other studies proposed that, AgNPs may attach to the surface of cell membrane disturbing permeability and respiration functions of the cell or by interfering with components of the microbial electron transport system [37, 38]. However, the mechanism of the bactericidal effect of AgNPs is not yet completely understood [18, 39].

Table 4: The antimicrobial activity (inhibition zone in mm) of the AgNPs synthesized against different strains before (B) and after (A) *in-vitro* gamma irradiation

Tested strains	*Tetracycline (Standard antibacterial agent)	*Amphotericin B (Standard antifungal agent)	**Diameter of inhibition zone (mm) produced by AgNPs		
			B Mean $\pm$ SD	A Mean $\pm$ SD	P-value
<i>Staphylococcus aureus</i> (MRSA)	26	--	27.67 $\pm$ 0.577	22.67 $\pm$ 1.155	0.0131•
<i>Staphylococcus epidermidis</i>	29	--	37.00 $\pm$ 2.646	31.33 $\pm$ 1.155	0.0422•
<i>Staphylococcus warneri</i>	30	--	28.67 $\pm$ 1.155	34.33 $\pm$ 3.055	0.0848
<i>Staphylococcus saprophyticus</i>	28	--	26.00 $\pm$ 1.000	21.67 $\pm$ 1.155	0.0390•
<i>Acinetobacter baumannii</i> / <i>haemolyticus</i>	27	--	17.33 $\pm$ 3.055	13.33 $\pm$ 0.577	0.1472
<i>Pseudomonas aeruginosa</i>	28	--	18.67 $\pm$ 2.082	20.33 $\pm$ 0.577	0.3377
<i>Klebsiella pneumonia</i>	30	--	19.67 $\pm$ 0.577	13.00 $\pm$ 1.000	0.0171•
<i>Escherichia coli</i>	32	--	21.67 $\pm$ 0.577	21.00 $\pm$ 1.000	0.1835
<i>Candida albicans</i>	--	19	31.33 $\pm$ 1.155	31.67 $\pm$ 0.577	0.4226
<i>Candida parapsilosis</i>	--	18	31.33 $\pm$ 1.155	37.33 $\pm$ 0.577	0.0267•
<i>Candida tropicalis</i>	--	20	34.00 $\pm$ 1.732	24.33 $\pm$ 0.577	0.0082•
<i>Candida glabrata</i>	--	16	35.33 $\pm$ 1.155	21.33 $\pm$ 1.155	0.0067•

\* Diameter of inhibition zone (mm).

\*\* Three repeats were performed for each tested strain

B: Before *in-vitro* gamma-irradiation. A: After *in-vitro* gamma-irradiation

•P- value significant &lt; 0.05

P- value non-significant &gt; 0.05

AgNPs (200ppm), concentration of antibiotics: 20 (ppm)

----- (not tested)

Table 5: Minimum inhibitory and minimum lethal concentration values of the AgNPs synthesized for the selected strains

Tested strains	MIC (ppm)		MIC <sub>50</sub> (ppm)		MIC <sub>90</sub> (ppm)		MLC (ppm)	
	B	A	B	A	B	A	B	A
<i>Staphylococcus aureus</i> (MRSA)	200	200	50	50	100	100	400	400
<i>Staphylococcus warneri</i>	200	100	50	50	100	100	200	200
<i>Acinetobacter baumannii</i> / <i>haemolyticus</i>	400	400	100	200	200	400	800	800
<i>Pseudomonas aeruginosa</i>	400	400	100	100	200	200	800	800
<i>Candida parapsilosis</i>	100	50	50	25	100	50	200	100

B: Before *in-vitro* gamma-irradiation A: After *in-vitro* gamma irradiation

It is possible that, AgNPs act similarly to the antimicrobial agents used for the treatment of bacterial infections, which show four different mechanisms of action including; interference with cell wall synthesis, inhibition of protein synthesis, interference with nucleic acid synthesis and inhibition of metabolic pathway [18]. Some studies have reported that, the positive charge on the Ag<sup>+</sup> ion is crucial for its antimicrobial activity through the electrostatic attractions between the negatively charged cell membrane of microorganisms and the positively charged nanoparticles [40-42]. In addition, AgNPs not only interact with the surface of membrane, but can also penetrate inside the bacteria [38]. AgNPs have also intensive tendency to react with sulfur and phosphorus groups, thus the cell membrane proteins containing sulfur and compounds containing phosphorus such as DNA are likely to be the preferential sites for AgNPs [43]. AgNPs have not been shown to

cause bacterial resistance currently complicating antibiotic therapy of bacterial infections. This is presumably due to the fact that, unlike antibiotics, AgNPs do not exert their antibacterial effects in a single specific site but at several levels such as bacterial wall, proteosynthesis and DNA (i.e. attack a broad range of targets in the organisms), which means that, microorganisms would have to develop a host of mutations simultaneously to protect themselves [44, 45]. Also, from the reported results the synthesized AgNPs exhibited a highly pronounced antifungal activity against yeast tested (Table 4), probably through destruction of yeasts potential and membrane integrity resulting in the formation of pores and cell death. Several other studies suggest that, inhibition of bud growth correlates with membrane damage and AgNPs inhibit the normal budding process through the destruction of membrane integrity [46].

Data in Table 4 clearly indicate that, the difference in the inhibitory action of AgNPs on MRSA, *Staphylococcus epidermidis*, *Staphylococcus saprophyticus*, *Klebsiella pneumonia*, *Candida parapsilosis*, *Candida tropicalis* and *Candida glabrata* before and after *in vitro* gamma irradiation was statistically significant (P-value<0.05). AgNPs inhibitory impact showed an increase after irradiation compared to before in case of *Staphylococcus warneri*, *Pseudomonas aeruginosa* and *Candida parapsilosis* probably due to the additional stress to the cells as a result of their exposure to low doses of ionizing radiation which tends to disturb their organization. However, due to the use of different methods of production, different nanoparticles size and different nanoparticles shape, many products commonly summarized under the name nanoparticles can be physically and chemically completely different preparations. Depending on these factors, nanoparticles can have highly variable antibacterial properties which result in controversial results [43, 47, 48]. It is reasonable to state that, the binding of the particles to the bacteria depends on the interaction of the surface area available. Smaller AgNPs having the larger surface area available for interaction would give more bactericidal effect than the larger AgNPs [49,50].

### CONCLUSION

Silver nanoparticles in the range of 14±4 nm are synthesized by the supernatant of *B. sterothermophilus* when silver nitrate is added to it. The silver nanoparticles synthesized are highly stable and this method has advantages over other methods as the organism used here is safe. This study would therefore lead to an easy procedure for producing silver nanoparticles with the added advantage of biosafety. The AgNPs synthesized exhibited remarkable antimicrobial activity against both Gram-positive and Gram-negative bacterial strains regardless of their drug-resistant mechanisms and also could be considered as a potential antifungal agent. The bactericidal and fungicidal activity have proved that AgNPs kill microorganisms at such low concentrations (units of ppm), which do not reveal acute toxic effects on human cells, in addition to overcoming resistance and lowering cost when compared to conventional antibiotics. The comparison of the antifungal activity of the AgNPs synthesized with their antibacterial activity clearly showed that the AgNPs inhibit yeast growth at lower concentrations than in the case of the bacterial growth inhibition. The variability of the values of the inhibition

activity of the AgNPs against bacteria and yeast tested before and after 24.41 Gy *in vitro* gamma irradiation could be strain-specific.

### ACKNOWLEDGMENTS

This work is a part of the Project "Nutraceuticals and Functional Foods Production by Using Nano/ Biotechnological and Irradiation Processes" and Nanotechnology Research Unit (P.I. Prof. Dr. Ahmed El-Batal) at Drug Microbiology Laboratory, the financial support provided by NCRRT. Also, this work is dedicated to ALSHAHEED /Mohamed El-Saeed Ezz Eldin Yasin (EGYPTIAN REVOLUTION, 25 January, 2011).

### REFERENCES

1. Huh, A.J. and Y.J. Kwon, 2011. Nanoantibiotics: a new paradigm for treating infectious diseases using nanomaterials in the antibiotics resistant era. *Journal of Controlled Release*, 156(2): 128-45.
2. Liao, S.Y., D.C. Read, W.J. Pugh, J.R. Furr and A.D. Russell, 1997. Interaction of silver nitrate with readily identifiable groups: relationship to the antibacterial action of silver ions. *Letters in Applied Microbiology*, 25(4): 279-283.
3. Gupta, A. and S. Silver, 1998. Molecular Genetics: Silver as a biocide: Will resistance become a problem? *Nature Biotechnology*, 16(10): 888.
4. Nomiya, K., A. Yoshizawa, K. Tsukagoshi, N.C. Kasuga, S. Hirakawa and J. Watanabe, 2004. Synthesis and structural characterization of silver (I), aluminium (III) and cobalt (II) complexes with 4-isopropyltropolone (hinokitiol) showing noteworthy biological activities. Action of silver (I)-oxygen bonding complexes on the antimicrobial activities. *Journal of Inorganic Biochemistry*, 98(1): 46-60.
5. Singh, M., S. Singh, S. Prasada and I. S. Gambhir, 2008. Nanotechnology in medicine and antibacterial effect of silver nanoparticles. *Digest Journal of Nanomaterials and Biostructures*, 3(3): 115-122.
6. Kalishwaralal, K., V. Deepak, S. Ramkumarpandian, H. Nellaiah and G. Sangiliyandi, 2008. Extracellular biosynthesis of silver nanoparticles by the culture supernatant of *Bacillus licheniformis*. *Materials Letters*, 62: 4411-4413.
7. Boyaci, I.H., 2005. A new approach for determination of enzyme kinetic constants using response surface methodology. *Biochemical Engineering Journal*, 25: 55-62.

8. Myers, R.H. and D.C. Montgomery, 2007. Response Surface Methodology: Process and Product Optimization Using Designed Experiment, John and Sons Inc., New York, NY.
9. Xiong, Y.H., J.Z. Liu, H.Y. Song and L.N. Ji, 2004. Enhanced production of extracellular ribonuclease from *Aspergillus niger* by optimization of culture conditions using response surface methodology. *Biochemical Engineering Journal*, 21(1): 27-32.
10. Shin, H.S., H.C. Choi, Y. Jung, S.B. Kim, H.J. Song and H.J. Shin, 2004. Chemical and size effects of nanocomposites of silver and polyvinyl pyrrolidone determined by X-ray photoemission spectroscopy. *Chemical Physics Letters*, 383: 418-422.
11. Senanayake, S.P.J. and F. Shahidi, 2002. Lipase-catalyzed incorporation of docosahexaenoic acid (DHA) into borage oil: optimization using response surface methodology. *Food Chemistry*, 77(1): 115-123.
12. Dey, G., A. Mitra, R. Banerjee and B.R. Maiti, 2001. Enhanced production of amylase by optimization of nutritional constituents using response surface methodology. *Biochemical Engineering Journal*, 7(3): 227-231.
13. El-Batal, A.I., A.A.M. Hashem and N.M. Abdelbaky, 2012. Enhancement of some natural antioxidants activity via microbial bioconversion process using gamma irradiation and incorporation into gold nanoparticles. *World Applied Sciences Journal*, 19(1): 01-11.
14. El-Batal, A. I., N.M. Thabet, A. Osman, A.R.B. Abdel Ghaffar and K.Sh. Azab, 2012. Amelioration of oxidative damage induced in gamma irradiated rats by nano selenium and lovastatin mixture. *World Applied Sciences Journal*, 19(7): 962-971.
15. El-Batal, A.I., O.A.R. Abou Zaid, E. Noaman and E.S. Ismail, 2012. Promising antitumor activity of fermented wheat germ extract in combination with selenium nanoparticles. *International Journal of Pharmaceutical Science and Health Care*, 6(2): 1-22.
16. El-Batal, A.I., O.A.R. Abou Zaid, E. Noaman and E.S. Ismail, 2012. *In vivo* and *in vitro* antitumor activity of modified citrus pectin in combination with selenium nanoparticles against Ehrlich carcinoma cells. *International Journal of Pharmaceutical Science and health Care*, 6(2): 23-47.
17. Krkljes, A.N., M.T. Marinovic-Cincovic, Z.M. Kacarevic-Popovic and J.M. Nedeljkovic, 2007. Radiolytic synthesis and characterization of Ag-PVA nanocomposites. *European Polymer Journal*, 43(6): 2171-2176.
18. Guzman, M., J. Dille and S. Godet, 2012. Synthesis and antibacterial activity of silver nanoparticles against Gram-positive and Gram-negative bacteria. *Nanomedicine: Nanotechnology, Biology and Medicine*, 8: 37-45.
19. Sadeghi, A., B. Rahimi and M. Shojapour, 2012. Molecular detection of metallo- $\beta$ -lactamase genes blaVIM-1, blaVIM-2, blaIMP-1, blaIMP-2 and blaSPM-1 in *Pseudomonas aeruginosa* isolated from hospitalized patients in Markazi province by Duplex-PCR. *African Journal of Microbiology Research*, 6(12): 2965-2969.
20. Vaidyanathan, R., S. Gopalram, K. Kalishwaralal, V. Deepak, S.R.K. Pandian and S. Gurunathan, 2010. Enhanced silver nanoparticle synthesis by optimization of nitrate reductase activity Colloids and Surfaces B: Biointerfaces, 75(1): 335-341.
21. Bauer, A.W., W.M.M. Kirby, J.C. Sherris and M. Truck, 1966. Antibiotic susceptibility testing by a standardized single disk method. *American Journal of Clinical Pathology*, 45(4): 493-496.
22. Barrow, G.I. and R.K.A. Feltham, 1993. Coawn and Steel's Manual for the Identification of Medical Bacteria. 3<sup>rd</sup> Ed., the Press Syndicate of the University of Cambridge, UK.
23. Fisher, F. and N.B. Cook, 1998. Fundamentals of Diagnostic Mycology. W.B. Saunders Company, Philadelphia.
24. Clinical and Laboratory Standard Institute (CLSI), 2008. Performance Standards for Antimicrobial Susceptibility Testing: Eighteenth Informational Supplement 18<sup>th</sup> ed., Clinical and Laboratory Standard Institute, USA (ISBN-13: 9781562386535).
25. Clinical and Laboratory Standard Institute (CLSI), 2009. Methods for Dilution of Antimicrobial Susceptibility Tests for Bacteria that Grow Aerobically. Approved Standard 5<sup>th</sup> ed. CLSI document; M07-A8 (ISBN 1-56238-689-1).
26. Ansari, M.A., H.M. Khan, A.A. Khan, A. Malik, A. Sultan, M. Shahid, F. Shujatullah and A. Azam, 2011. Evaluation of antibacterial activity of silver nanoparticles against MSSA and MRSA on isolates from skin infections. *Biology and Medicine*, 3(2): 141-146.
27. Barton, M.F.R., 1995. Tables of equivalent dose in 2 Gy fractions: A simple application of the linear quadratic formula. *International Journal of Radiation Oncology Biology Physics*, 31(2): 371-378.



28. Myers, R.H. and R.C. Montgomery, 2002. Response Surface Methodology: Process and Product Optimization Using Designed Experiments. New York: Wiley.
29. Majeed, K.M.A., K. Sushil, A. Maqsood, A.A. Salman, M.S. Alsalhi, A. Mansour and A.S. Aldwayyan, 2011. Structural and spectroscopic studies of thin film of silver nanoparticles. Applied Surface Science, 257(24): 10607-10612.
30. Marignier, J.L., J. Belloni, M.O. Delcourt and J.P. Chevalier, 1985. Microaggregates of non-noble metals and bimetallic alloys prepared by radiation-induced reduction. Nature, 317: 344-345.
31. Sheikh, N., A. Akhavan and M.Z. Kassaee, 2009. Synthesis of antibacterial silver nanoparticles by Gamma-irradiation. Physica E, 42(2): 132-135.
32. Morones, J.R., J.L. Elechiguerra, A. Camacho, K. Holt, J.B. Kouri, J.T. Ramírez and M.J. Yacaman, 2005. The bactericidal effect of silver nanoparticles. Nanotechnology, 16(10): 2346-2353.
33. Rai, M., A. Yadav and A. Gade, 2009. Silver nanoparticles as a new generation of antimicrobials. Biotechnology Advances, 27(1): 76-83.
34. Huang, L., T. Dai, Y. Xuan, G.P. Tegos and M.R. Hamblin, 2011. Synergistic combination of chitosan acetate with nanoparticle silver as a topical antimicrobial: Efficacy against bacterial burn infections. Antimicrobial Agents and Chemotherapy, 55(7): 3432-3438.
35. Ayala-Nunez, N.V., H.H.L. Villegas, C.I. Turrent and C.R. Padilla, 2009. Silver nanoparticles toxicity and bactericidal effect against methicillin-resistant *Staphylococcus aureus*: Nanoscale does matter. Nanobiotechnology, 5(1-4): 2-9.
36. Yamanaka, M., K. Hara and J. Kudo, 2005. Bactericidal actions of a silver ion solution on *Escherichia coli* studied by energy filtering transmission electron microscopy and proteomic analysis. Applied and Environmental Microbiology, 71(11): 7589-7593.
37. Percival, S.L., P.G. Bowler and D. Russell, 2005. Bacterial resistance to silver in wound care. Journal of Hospital Infection, 60(1): 1-7.
38. Sharma, V.K., R.A. Yngard and Y. Lin, 2009. Silver nanoparticles: Green synthesis and their antimicrobial activities. Advances in Colloid and Interface Science, 145: 83-96.
39. Ketchart, O., A. Treetong, P. Na-Ubon and N. Supaka, 2012. Determination of the effect of silver nanoparticles on Gram-positive bacterial cells by atomic force microscopy. Advanced Materials Research, 506: 202-205.
40. Soni, I. and B. Salopek-Soni, 2004. Silver nanoparticles as antimicrobial agent: a case study on *E. coli* as a model for Gram-negative bacteria. Journal of Colloid and Interface Science, 275(1): 177-182.
41. Tiwari, D.K., J. Behari and P. Sen, 2008. Time and dose dependent antimicrobial potential of Ag nanoparticles synthesized by top-down approach. Current Science, 95(5): 647-655.
42. Vijayakumar, M., K. Priya, F.T. Nancy, A. Noorlidah and A.B.A. Ahmed, 2013. Biosynthesis, characterization and anti-bacterial effect of plant-mediated silver nanoparticles using *Artemisia nilagirica*. Industrial Crops and Products, 41: 235-240.
43. Dehkordi, S.H., F. Hosseinpour and A.E. Kahrizangi, 2011. An *in vitro* evaluation of antibacterial effect of silver nanoparticles on *Staphylococcus aureus* isolated from bovine subclinical mastitis. African Journal of Biotechnology, 10(52): 10795-10797.
44. Parameswari, E., C. Udayasoorian, S.P. Sebastian and R.M. Jayabalakrishnan, 2010. The bactericidal potential of silver nanoparticles. International Research Journal of Biotechnology, 1(3): 044-049.
45. Nasrollahi, A., K.H. Pourshamsian and P. Mansourkiaee, 2011. Antifungal activity of silver nanoparticles on some fungi. International Journal of Nano Dimension, 1(3): 233-239.
46. Merisko-Liversidge, E., G.G. Liversidge and E.R. Cooper, 2003. Nanosizing: A formulation approach for poorly-water-soluble compounds. European Journal of Pharmaceutical Sciences, 18(2): 113-120.
47. Pal, S., Y.K. Tak and J.M. Song, 2007. Does the antibacterial activity of silver nanoparticles depend on the shape of the nanoparticle? A study of the Gram-negative bacterium *Escherichia coli*. Applied and Environmental Microbiology, 73(6): 1712-1720.
48. Shrivastava, S., T. Bera, A. Roy, G. Singh, P. Ramachandrarao and D. Dash, 2007. Characterization of enhanced antibacterial effects of novel silver nanoparticles. Nanotechnology, 18: 225103 (9pp).
49. Fayaz, A.M., K. Balaji, M. Girilal, R. Yadav, P.T. Kalaichelvan and R. Venketesan, 2010. Biogenic synthesis of silver nanoparticles and their synergistic effect with antibiotics: a study against Gram-positive and Gram-negative bacteria. Nanomedicine: Nanotechnology, Biology and Medicine, 6(1): 103-109.